SCIENTIFIC REPORTS

OPEN

A novel violet/blue light-emitting device based on $Ce_2Si_2O_7$

Ling Li, Shenwei Wang, Guangyao Mu, Xue Yin, Kai Ou & Lixin Yi

Received: 07 April 2015
Accepted: 19 October 2015
Published: 13 November 2015

Rare-earth silicates are highly efficient materials for silicon-based light sources. Here we report a novel light-emitting device based on $Ce_2Si_2O_7$. Intense violet/blue electroluminescence was observed, with a turn-on voltage of about 13V. The violet/blue emission is attributed to 4f–5d transitions of the Ce^{3+} ions in $Ce_2Si_2O_7$, which are formed by interfacial reaction of CeO_2 and Si. Electroluminescence and photoluminescence mechanisms of the $Ce_2Si_2O_7$ light-emitting device are also discussed.

Silicon-based light-emitting devices have attracted considerable attention, since silicon has many advantages such as low fabrication cost, mature fabrication and processing technology, and high electrical and thermal conductivities[1]. In the past decades, integrations of ZnO, GaN, and other III-V semiconductors with silicon were extensively studied for novel optoelectronic applications because of the direct and wide band gaps of these materrials[2–4]. However, the lattice and thermal mismatch between these materials and Si still presents a significant challenge[5,6]. Alternatively, rare-earth doped SiO_2 has attracted a lot of interest due to their high luminescence efficiency and wide spectral range spanning from ultraviolet (UV) to infrared (IR). More importantly, SiO_2 is naturally compatible with Si technology[7,8]. Previously, efficient visible light-emitting devices based on rare-earth doped metal-oxide-semiconductor (MOS) structures have been demonstrated[9–11]. However, the solubility of rare-earth ions in Si-based materials achieved so far is still relatively low ($10^{16}–10^{20}\,cm^{-3}$)[12]. In fact, even if the solubility could be improved, since the rare-earth ions (e.g. Er^{3+}, Eu^{3+}, Ce^{3+}) are optically inactive at high concentrations due to the formation of clusters[13–15], such a concentration quenching would still be a significant barrier for further improving performance of rare-earth doped Si-based materials. Recently, it was shown that formation of rare-earth silicates (e.g. Er_2SiO_5, Eu_2SiO_5, $Ce_2Si_2O_7$) could enhance their photoluminescence efficiency[16–18]. It was found that in these silicates, the rare-earth ions are 100% activated, and the solubility can reach $10^{22}\,cm^{-3}$[19–21].

$Ce_2Si_2O_7$ is a promising material for UV optoelectronic devices, with an emission band similar to that of ZnO and GaN. In addition, different emission wavelengths could be obtained from the energy transfer between Ce^{3+} and other rare-earth ions (such as Er^{3+}, Tb^{3+}, Dy^{3+}, Sm^{3+})[10,11,22,23]. Although photoluminescence (PL) of $Ce_2Si_2O_7$ has been investigated by several groups[16,18,24,25], there has been no reports on electroluminescence (EL) of $Ce_2Si_2O_7$ so far. In this paper, $Ce_2Si_2O_7$ is synthesized by interfacial reaction of CeO_2 thin film and Si wafer in reducing ambient. Violet/blue emissions at about 390 and 410 nm from $Ce_2Si_2O_7$ were obtained. The internal quantum efficiency of $Ce_2Si_2O_7$ was found to be about 37% at room temperature. Finally, we fabricated $Ce_2Si_2O_7$ light-emitting devices (LEDs), and achieved a turn on voltage of 13 V, while the maximum EL intensity was obtained at a driving voltage of 25 V.

Results and Discussion

In order to investigate the effect of annealing ambient on the structural change of CeO_2 films, X-ray diffraction (XRD) patterns of as-deposited and annealed CeO_2 films were measured. As shown in Fig. 1(a), the crystal structure of the samples depends strongly on the annealing ambient. The as-deposited film contains a broad reflection around 28.6°, which corresponds to the (111) plane of CeO_2. When the as-deposited film was annealed in O_2 ambient, the diffraction peak at 28.6° becomes higher and narrower, and the (200) plane of CeO_2 can be identified. The $Ce_2Si_2O_7$ phase is obtained after the as-deposited CeO_2 film was annealed in reducing ambient, and the highest reflection peak is identified as the (008)

Key Laboratory of Luminescence and Optical Information, Ministry of Education, Institute of Optoelectronic Technology, Beijing Jiaotong University, Beijing, 100044, China. Correspondence and requests for materials should be addressed to L.Y. (email: lxyi@bjtu.edu.cn)

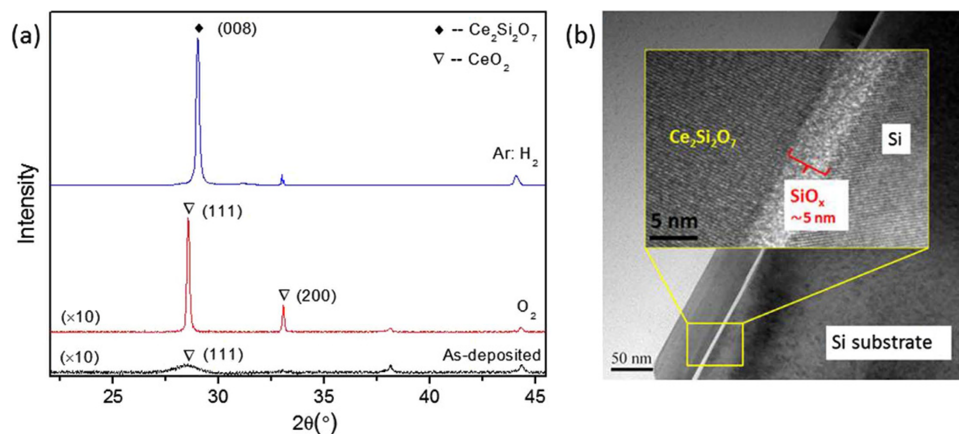

Figure 1. (a) XRD of as-deposited and annealed CeO_2 films at 1060 °C for 1 hour, (b) TEM image of the $Ce_2Si_2O_7$ film. The inset shows high-magnification TEM of the interface region marked by the yellow box.

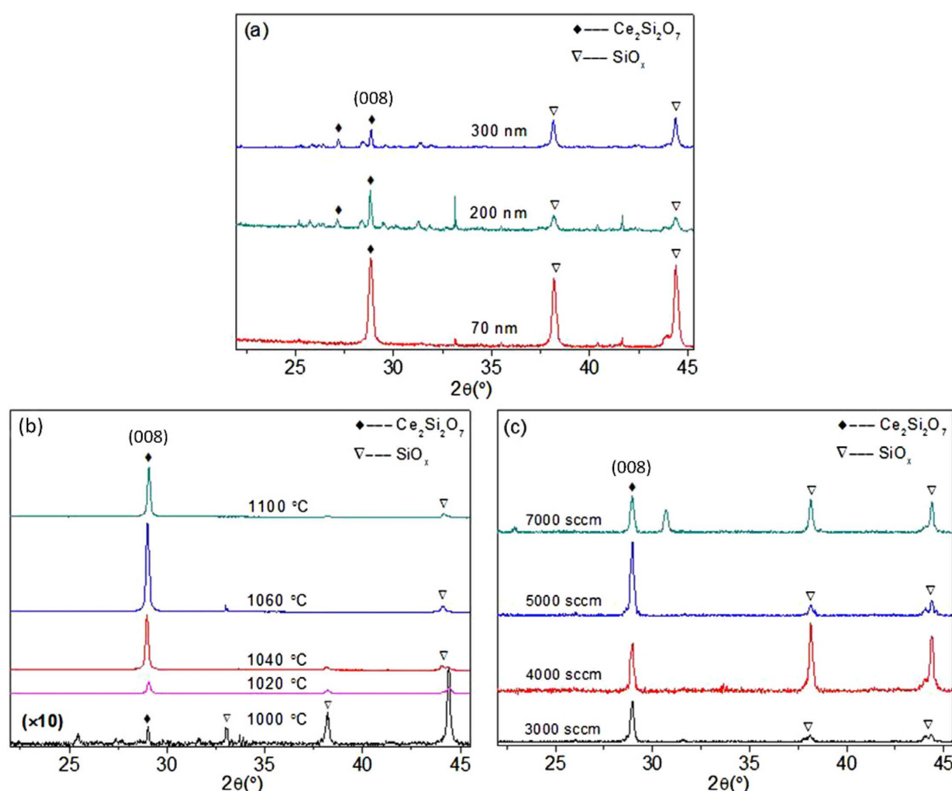

Figure 2. (**a**) XRD of as-deposited CeO_2 films with different thicknesses annealed at 1020 °C for 1 hour, (**b**) XRD of 70 nm CeO_2 films annealed at various temperatures for 1 hour, (**c**) XRD of 70 nm CeO_2 films annealed at 1040 °C by different annealing ambient flow rate.

plane. The lattice structure is also investigated by transmission electron microscopy (TEM). As shown in Fig. 1(b), the thickness of $Ce_2Si_2O_7$ is about 50 nm. There is an amorphous SiO_x layer at the $Ce_2Si_2O_7$/Si interface, with a thickness of about 5 nm. During the annealing process, CeO_2 was reduced to CeO_{2-x}, while Si was oxidized. Then, SiO_x and CeO_{2-x} reacted at high temperature, resulting in $Ce_2Si_2O_7$ with various crystallographic orientations.

The lattice structure of $Ce_2Si_2O_7$ observed is different from previous reports[18,26,27]. We attribute this to the strong dependence of the crystallinity and orientation on deposition and annealing conditions[27–29]. To confirm this, the as-deposited CeO_2 films with different thicknesses were annealed in reducing ambient ($Ar:H_2 = 97:3$) for 1 hour. As shown in Fig. 2(a), there are various crystallographic orientations of $Ce_2Si_2O_7$ when 300 nm CeO_2 film was annealed at 1020 °C. However, the intensity of the (008) diffraction

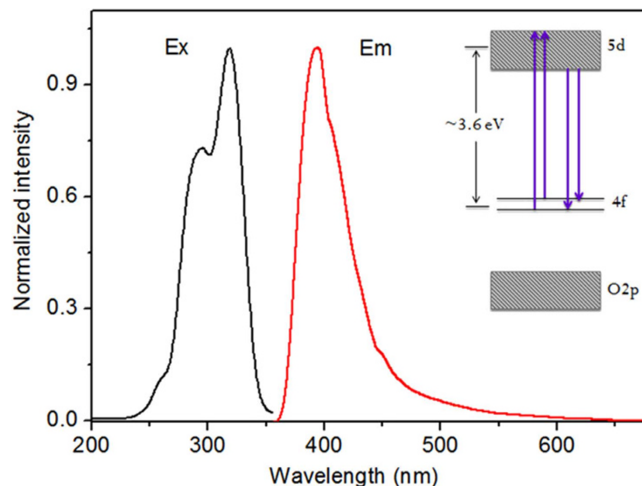

Figure 3. PL and PLE spectra of the CeO_2 film annealed in Ar:H_2 ambient with the excitation wavelength of 325 nm, the PLE was measured with a detection wavelength of 390 nm. The inset shows the energy levels diagram of $Ce_2Si_2O_7$. All the spectra were measured at room temperature.

peak increases with decreasing the thickness of CeO_2. In Fig. 2(b), various crystallographic orientations of $Ce_2Si_2O_7$ are exhibited when a 70 nm CeO_2 film was annealed at 1000 °C. Unlike the 300 nm film, here the (008) diffraction peak initially increases with the annealing temperature up to 1020 °C, and then decreases while the annealing temperature is further raised to above 1060 °C. Similarly, as shown in Fig. 2(c), this peak first increases with the annealing ambient flow rate is increased, and then decreases once the flow rate up is above 5000 sccm. In summary, these observations show that the deposition and annealing conditions are critical factors for synthesizing $Ce_2Si_2O_7$.

Figure 3 shows the PL spectrum of the CeO_2 film annealed in Ar:H_2 ambient. The intense violet/blue emission consists of two peaks centered at about 390 nm (3.18 eV) and 410 nm (3.02 eV), respectively. Both the shape and the position of the peaks are similar to the results obtained by Choi[18]. However, these emission bands are not observed in the as-deposited films or the samples annealed in O_2 ambient. Combined with crystal structure analysis mentioned above, the violet/blue emission bands are attributed to the formation of $Ce_2Si_2O_7$, and correspond to the Ce^{3+} transitions from the relaxed lowest 5d excited state to 4f ground states. The energy separation of the two peaks is about 2000 cm^{-1}, which matches well with the theoretical value of spin–orbit splitting between the 4f ground state $^2F_{5/2}$ and $^2F_{7/2}$[30]. The excitation bands located at 295 nm (4.2 eV) and 324 nm (3.83 eV) can be assigned to the 4f–5d transitions[31]. Based on these assignments, a simplified energy level diagram is sketched in Fig. 3. In order to estimate the optical band gap (E_g^{opt}) of $Ce_2Si_2O_7$, we measured the absorption spectrum of the sample in the visible range, and obtain a value of 3.6 eV by extrapolating the spectrum using Tauc's relation[32]:

$$(\alpha h\nu)^2 = C\left(h\nu - E_g{}^{opt}\right) \tag{1}$$

where α is the absorption coefficient, h is the Planck's constant, ν is the photon frequency, and C is a constant.

According to several previous studies, Ce^{3+} activator concentration is limited to about 0.5 at% in most host materials[33–35]. However, our results show that Ce^{3+} ions in $Ce_2Si_2O_7$ are almost 100% activated. This is similar to self-activated materials such as CeF_3 and $CeCl_3$[36]. We find that Ce^{3+} emission is enhanced significantly by the formation of $Ce_2Si_2O_7$. To quantify this enhancement, we measured the internal quantum efficiency of $Ce_2Si_2O_7$ by using an integrated sphere[37]. We obtained a value of about 37% at room temperature. To reveal the excitation and emission mechanisms, we measured the PL spectra as a function of temperature. As shown in Fig. 4, the PL intensity increases as the sample temperature is decreased. We also measured PL decay time at temperatures of 77 and 300 K, respectively, as shown in the inset of Fig. 4. The PL decays exponentially, with the time constant slightly changes from 17 to 21 ns as the temperature is decreased from 300 to 77 K. This very short lifetime is in agreement with the electric-dipole allowed 4f–5d transition rate of Ce^{3+}. Since non-radiative centers are frozen at low temperatures, we attribute the decrease of the PL intensity and the decay time to the energy transfer to defect centers by non-radiative recombination processes[38].

Next, we fabricated $Ce_2Si_2O_7$ LEDs with the structure diagram shown in Fig. 5. Violet/blue EL emission is clearly observed when a positive voltage is applied on the indium tin oxide (ITO) layer. The turn-on voltage of the device is found to be as low as 13 V. The EL spectra (Fig. 5) are in good agreement with the PL spectra (Fig. 3). The EL intensity increases with the forward voltage, and the maximum EL

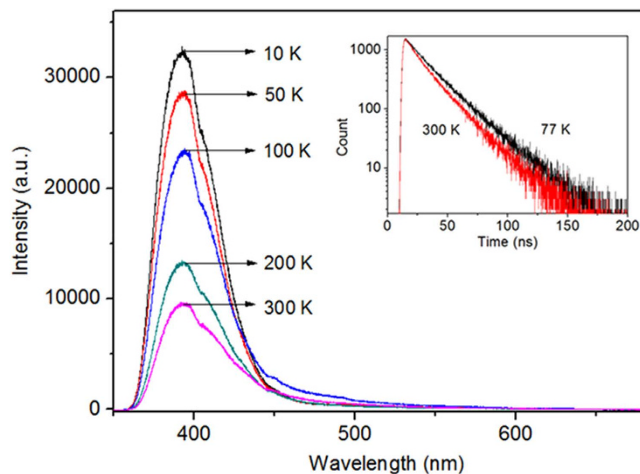

Figure 4. PL spectra from $Ce_2Si_2O_7$ in the temperature range from 10 to 300 K with the excitation wavelength of 325 nm. The inset shows the PL decay of $Ce_2Si_2O_7$.

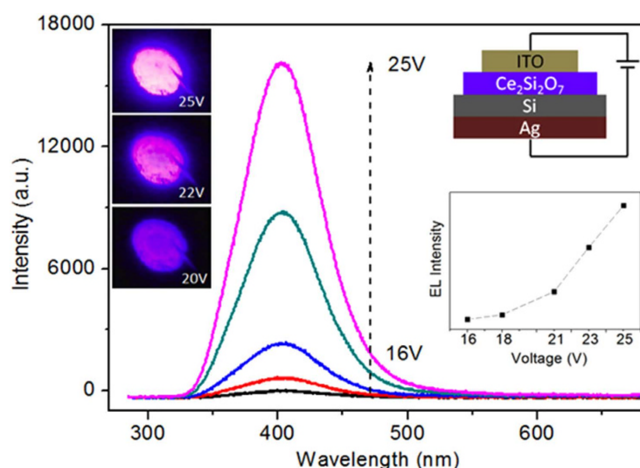

Figure 5. EL spectra of the LED at various forward biases of 16–25 V. The insets show the structure diagram of the LED and EL photos of the device at different voltages.

intensity is obtained at 25 V. Figure 6 presents a typical current-voltage (I-V) characteristics. The forward current of the device reaches up to 0.26 mA when the forward bias is 25 V, while a reverse leakage current of 6.4 μA at a bias voltage of −10 V is observed. These values illustrate the excellent rectification performance achieved in this device.

Based on the energy level diagram of $Ce_2Si_2O_7$ developed in this work, we propose the following mechanism of the LED operation: As seen from the inset of Fig. 6, an asymmetrical energy barrier is formed at the junction interface. When a positive voltage is applied between the two electrodes (forward bias), the electrons accumulated in the Si/SiO_x interface are swept to $Ce_2Si_2O_7$ side by tunneling through the SiO_x barrier. Meanwhile, the holes are injected into $Ce_2Si_2O_7$ from ITO and accumulated at $Ce_2Si_2O_7$/SiO_x interface due to the SiO_x barrier. As a result, the EL originates from the recombination between the injected electrons and holes in $Ce_2Si_2O_7$. These emitted photons with an energy (hυ) approximately equals to the energy difference between 4f and 5d states of Ce^{3+}. Hence, in this design, the SiO_x layer functions as a carrier blocking layer. For high-performance and reliable device operation, the ideal thickness of SiO_x layer should be less than 2 nm[39]. Therefore, the turn-on voltage can be further decreases, considering the 5 nm SiO_x layer used in this device.

In summary, a new method of synthesizing $Ce_2Si_2O_7$ was demonstrated. $Ce_2Si_2O_7$ was formed after the Si-based CeO_2 film was annealed in reducing ambient. Intense violet/blue emission was observed from $Ce_2Si_2O_7$, and the PL emission bands are located around 390 and 410 nm, which are attributed to 4f–5d transitions of Ce^{3+}. More importantly, $Ce_2Si_2O_7$ LEDs were fabricated and strong violet/blue EL emission was observed. The turn on voltage of $Ce_2Si_2O_7$ LED is 13 V and the maximum EL intensity was obtained at 25 V.

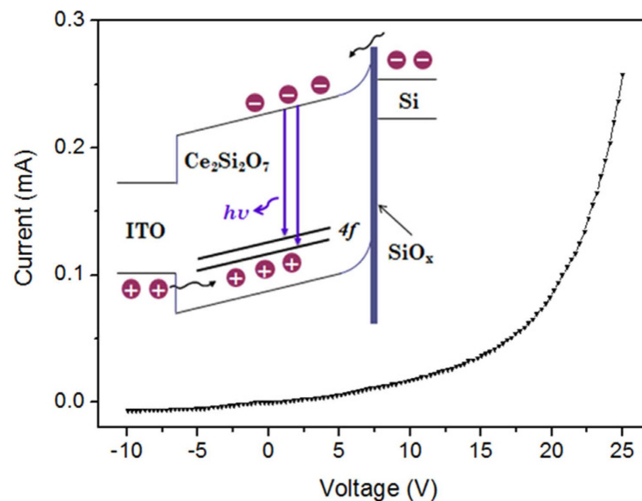

Figure 6. Current-voltage characteristic of the device. The inset shows the energy band diagram of the devices and the charge transfer process.

Methods

CeO_2 thin films were deposited on P-type Si (100) substrates by electron beam evaporation (EVA 450). The as-deposited films were annealed in reducing ambient ($Ar:H_2 = 97:3$) at various temperatures for 1 hour. We fabricated the LEDs as schematically illustrated in the inset of Fig. 5. ITO and Ag electrodes were deposited on the surface of the film and the back side of Si substrates, respectively, both by magnetron sputtering. The PL spectra were measured by a He-Cd laser with a 325 nm excitation wavelength, and the PL excitation (PLE) spectrum was measured with a fluorescence spectrometer (FLS920) using a 450 W xenon lamp as the excitation source. The crystal structures were characterized by XRD using Cu Kα radiation (Bruker D8 ADVANCE), and morphology of the samples was determined by TEM (Hitachi, H8100 200 kV). The internal quantum efficiency of samples is measured using an F-3018 integrating sphere with a 335 nm laser excitation. The PL decay was measured by using a nanosecond xenon flash lamp at 325 nm excitation wavelength and detected by a time-correlated single photon-counting system. The EL spectra of the devices and I-V characteristics were measured by a system of an ACTON 150 CCD spectrometer and a Keithley 2410, respectively.

References

1. Hirschman, K. D., Tsybeskov, L., Duttaguptap, S. P. & Fauchet, M. Silicon-based visible light-emitting devices integrated into microelectronic circuits. *Nature* **384,** 338–341 (1996).
2. Nguyen, H. P. T. *et al.* p-Type Modulation Doped InGaN/GaN Dot-in-a-Wire White-Light-Emitting Diodes Monolithically Grown on Si(111). *Nano Lett.* **11,** 1919–1924 (2011).
3. Hsieh, Y. P. *et al.* Electroluminescence from ZnO/Si-nanotips light-emitting diodes. *Nano Lett.* **9,** 1839–1843 (2009).
4. Ra, Y. H., Navamathavan, R., Park, J. H. & Lee, C. R. High-Quality Uniaxial $In_xGa_{1-x}N$/GaN Multiple Quantum Well (MQW) Nanowires (NWs) on Si(111) Grown by Metal-Organic Chemical Vapor Deposition (MOCVD) and Light-Emitting Diode (LED) Fabrication. *ACS Appl. Mater. Interfaces* **5,** 2111–2117 (2013).
5. Xiong, C. *et al.* Integrated GaN photonic circuits on silicon (100) for second harmonic generation. *Opt. Express* **19,** 10462–10470 (2011).
6. Triviño, N. V. *et al.* Integrated photonics on silicon with wide bandgap GaN semiconductor. *Appl. Phys. Lett.* **102,** 081120 (2013).
7. Rebohle, L. *et al.* Strong electroluminescence from SiO_2-Tb_2O_3-Al_2O_3 mixed layers fabricated by atomic layer deposition. *Appl. Phys. Lett.* **104,** 251113 (2014).
8. Izeddin, I., Moskalenko, A. S., Yassievich, I. N., Fujii, M. & Gregorkiewicz, T. Nanosecond Dynamics of the Near-Infrared Photoluminescence of Er-Doped SiO_2 Sensitized with Si Nanocrystals. *Phys. Rev. Lett.* **97,** 207401 (2006).
9. Sun, J. M. *et al.* Efficient ultraviolet electroluminescence from a Gd-implanted silicon metal-oxide-semiconductor device. *Appl. Phys. Lett.* **85,** 3387–3389 (2004).
10. Sun, J. M., Skorupa, W., Dekorsy, T., Helm, M. & Nazarov, A. N. The effect of annealing conditions on the crystallization of Er-Si-O formed by solid phase reaction. *Opt. Mater.* **27,** 1050–1054 (2005).
11. Sun, J. M. *et al.* Bright green electroluminescence from Tb^{3+} in silicon metal-oxide-semiconductor devices. *J. Appl. Phys.* **97,** 123513 (2005).
12. Polman, A. *et al.* A. Erbium in crystal silicon limits. *J. Appt. Phys.* **77,** 1256–1262 (1995).
13. Watras, A., Dereń, P. J. & Pąik, R. Luminescence properties and determination of optimal RE^{3+} (Sm^{3+}, Tb^{3+} and Dy^{3+}) doping levels in the KYP_2O_7 host lattice obtained by combustion synthesis. *New J. Chem.* **38,** 5058–5068 (2014).
14. Hori, Y. *et al.* GaN quantum dots doped with Tb. *Appl. Phys. Lett.* **88,** 053102 (2006).
15. Xia, Z. G. & Liu, R. S. Tunable Blue-Green Color Emission and Energy Transfer of $Ca_2Al_3O_6F:Ce^{3+}$, Tb^{3+} Phosphors for Near-UV White LEDs. *J. Phys. Chem. C* **116,** 15604–15609 (2012).
16. Choi, H. J. *et al.* Self-Organized Growth of Si/Silica/$Er_2Si_2O_7$ Core-Shell Nanowire Heterostructures and their Luminescence. *Nano Lett.* **5,** 2432–2437 (2005).
17. Savio, R. L. *et al.* Enhanced 1.54 μm emission in Y-Er disilicate thin films on silicon photonic crystal cavities. *Opt. Express* **21,** 10278–10288 (2013).
18. Choi, W. C. *et al.* Violet/blue light-emitting cerium silicates. *Appl. Phys. Lett.* **75,** 2389–2391 (1999).

19. Miritello, M. *et al.* Efficient Luminescence and Energy Transfer in Erbium Silicate Thin Films. *Adv. Mater.* **19,** 1582–1588 (2007).
20. Masaki, K., Isshiki, H., Kawaguchi, T. & Kimura, T. The effect of annealing conditions on the crystallization of Er-Si-O formed by solid phase reaction. *Opt. Mater.* **28,** 831–835 (2006).
21. Isshiki, H., Dood, M. J. A., Polman, A. & Kimura, T. Self-assembled infrared-luminescent Er-Si-O crystallites on silicon. *Appl. Phys. Lett.* **85,** 4343–4345 (2004).
22. Li, L. *et al.* Investigation on white light emissions from CeO_2/Dy_2O_3 multilayer films based on silicon substrates. *Vacuum* **112,** 38–41 (2015).
23. Li, L. *et al.* Investigation on photoluminescence properties of CeO_2/Sm_2O_3 multilayer films based on Si substrates. *Phys. Status Solidi B.* **251,** 737–740 (2014).
24. Kepinski, L., Hreniak, D. & Strek, W. Microstructure and luminescence properties of nanocrystalline cerium silicates. *J. Alloy Compd.* **341,** 203–207 (2002).
25. Li, J. *et al.* The formation of light emitting cerium silicates in cerium-doped silicon oxides. *Appl. Phys. Lett.* **94,** 011112 (2009).
26. Quah, H. J. *et al.* Effects of Postdeposition Annealing in Argon Ambient on Metallorganic Decomposed CeO2 Gate Spin Coated on Silicon. *J. Electrochem Soc.* **157,** 6–12 (2010).
27. Kepinski, L., Wolcyrz, M. & Marchewka, M. Structure Evolution of Nanocrystalline CeO2 Supported on Silica: Effect of Temperature and Atmosphere. *J. Solid State Chem.* **168,** 110–118 (2002).
28. Mamatrishat, M. *et al.* Valence number transition and silicate formation of cerium oxide films on Si(100). *Vacuum* **86,** 1513–1516 (2012).
29. Pagliuca, F., Luches, P. & Valeri, S. Interfacial interaction between cerium oxide and silicon surfaces. *Surf. Sci.* **607,** 164–169 (2013).
30. Dieke, G. H. *Spectra and Energy Levels of Rare Earth Ions in Crystals* (Plenum Publications, New York, 1968).
31. Skorodumova, N. V. *et al.* Electronic, bonding, and optical properties of CeO_2 and Ce_2O_3 from first principle. *Phys. Rev. B* **64,** 115108 (2001).
32. Tauc, J., Grigorovici, R. & Vancu, A. Optical Properties and Electronic Structure of Amorphous Germanium. *Phys. Stat. Sol.* **15,** 627–637 (1966).
33. Koao, L. F., Swart, H. C., Obed, R. I. & Dejene, F. B. Synthesis and characterization of Ce^{3+} doped silica (SiO_2) nanoparticles. *J. Lumin.* **131,** 1249–1254 (2011).
34. Katelnikovas, A. *et al.* Photoluminescence in sol-gel-derived YAG:Ce phosphors. *J. Cryst. Growth* **304,** 361–368 (2007).
35. Feng, H., Ding, D. Z. & Li, H. Cerium concentration and temperature dependence of the luminescence of $Lu_2Si_2O_7$:Ce scintillator. *J. Alloy Compd.* **509,** 3855–3858 (2011).
36. Li, Y. & Yan, B. Functionalized Mesoporous SBA-15 with CeF_3: Eu^{3+} Nanoparticle by Three Different Methods: Synthesis, Characterization, and Photoluminescence. *Nanoscale Res. Lett.* **5,** 701–708 (2010).
37. Mello, J. C., Wittmann, H. F. & Friend, R. H. An improved experimental determination of external photoluminescence quantum efficiency. *Adv. Mater.* **9,** 230–232 (1997).
38. Lee, B. G. *et al.* Strained Interface Defects in Silicon Nanocrystals. *Adv. Funct. Mater.* **22,** 3223–3232 (2012).
39. Alers, G. B. *et al.* Intermixing at the tantalum oxide/silicon interface in gate dielectric structures. *Appl. Phys. Lett.* **73,** 1517–1519 (1998).

Acknowledgements
This work was financially supported by the National Science Foundation of China (Grant no. 60977017, 61275058) and the Fundamental Research Funds for the Central Universities (2013JBM101).

Author Contributions
L.X.Y. conceived the idea and designed the study. L.L. carried out experiments and wrote the manuscript. L.L., S.W.W., G.Y.M., X.Y., K.O. and L.X.Y. discussed the results and commented the manuscript.

Additional Information
Competing financial interests: The authors declare no competing financial interests.

How to cite this article: Li, L. *et al.* A novel violet/blue light-emitting device based on $Ce_2Si_2O_7$. *Sci. Rep.* **5**, 16659; doi: 10.1038/srep16659 (2015).

This work is licensed under a Creative Commons Attribution 4.0 International License. The images or other third party material in this article are included in the article's Creative Commons license, unless indicated otherwise in the credit line; if the material is not included under the Creative Commons license, users will need to obtain permission from the license holder to reproduce the material. To view a copy of this license, visit http://creativecommons.org/licenses/by/4.0/